PAN ARCHIVES OF ACOUSTICS
Vol. **43**, No. 3, pp. 487–495 (2018)

DOI: 10.24425/123920

Amelioration of Ultrasonic Transducer to Study CuO Doped Thin Films

Mirham A.Y. BARAKAT[(1), (2)]

[(1)] *Ultrasonic Department*
National Institute of Standards
P.O. Box: 136, Giza code 12211, Tersa Street, Haram, Giza, Egypt

[(2)] *Physics Department, Faculty of Science, Hail University*
Hail, Saudi Arabia; e-mail: mirham75@yahoo.com

(*received May 8, 2017; accepted April 11, 2018*)

Ultrasonic pulse echo technique was used to study cupric oxide (CuO) thin films. CuO thin films were prepared using sol gel technique. They were doped with Lithium (Li) (1%, 2% and 4%).

Thin films' thickness (d) and band gap energy (E_g) were measured. In addition, elastic moduli (longitudinal (L), shear (G), bulk (K) and Young's (E)) and Poisson's ratio (v) were determined to estimate the microstructure properties of the prepared films.

The study ameliorated the used transducers to overcome their dead zone and beam scattering; wedges were developed. The results showed the effectiveness of these wedges. They enhanced transducers' sensitivity by changing the dead zone, beam diameter, beam directivity and waves' transmission.

Also, the study noted that Li doping caused the improvement of CuO thin films to be more useful in solar cell fabrication. Li-CuO thin films had narrower band gap. Thus, they acquired a high quantum yield for the excited carriers; also they gained more efficiency to absorb solar light.

Keywords: ultrasonic; thin films; doping; microstructure; wedges.

1. Introduction

1.1. Ultrasonic test principle

Ultrasonic is one of the most applied processes of non-destructive testing. Ultrasonic beam transmitted into the specimen under test will be reflected to the transducer and converted to an electric impulse due to piezo-electric effect. This impulse is displayed on the screen of the flaw detector apparatus. From the displayed impulse echoes many factors can be determined such as specimen thickness, ultrasonic velocity in the specimen, ultrasonic attenuation, etc.

Ultrasonic can give valuable information about the microstructure properties of the materials. From ultrasonic velocities (e.g. longitudinal, C_L and shear velocities, C_S), we can determine several important material properties, such as elastic moduli and Poisson's ratio.

The ultrasonic velocity (C) in the material can be obtained from the transit time (Δt) and the specimen's thickness (d) (Gaafar *et al.*, 2013).

$$C = \frac{2d}{\Delta t}. \tag{1}$$

The elastic moduli (longitudinal (L), shear (G), bulk (K) and Young's (E)) and Poisson's ratio (v) can be determined as follow:

$$L = \rho\,(C_L)^2\,, \tag{2}$$

$$G = \rho\,(C_S)^2\,, \tag{3}$$

$$K = L - \frac{4}{3}G, \tag{4}$$

$$v = \frac{1 - 2\left(\frac{C_S}{C_L}\right)^2}{2 - 2\left(\frac{C_S}{C_L}\right)^2}, \tag{5}$$

$$E = 2\rho\,(C_S)^2\,(1+v)\,, \tag{6}$$

where ρ is the density.

Thus, given measurements of ρ, C_L, and C_S, it is possible to determine all last cited parameters (Matori *et al.*, 2010).

1.2. Copper oxide thin films

Thin films made from oxide materials have good flexibility and they are used in electronic device applications as well as solar cell technology (Chopra *et al.*, 2004; Katz *et al.*, 2002).

There are two stable oxides of copper: copper (II) oxide (CuO) and copper (I) oxide (Cu_2O). CuO belongs to the monoclinic crystal system. The copper atom is coordinated by 4 oxygen atoms in an approximately square planar configuration.

CuO is a p-type semiconductor, with a narrow band gap of 1.2–1.5 eV (Forsyth, Hul, 1991; Saravanakannan, Radhakrishnan, 2014). It is an amphoteric oxide, so it dissolves in mineral acids such as hydrochloric acid, sulfuric acid or nitric acid to give the corresponding copper (II) salts (Richardson *et al.*, 2001).

CuO is an attractive material because the non-toxicity, abundant availability, low production cost and p-type conductivity. Therefore, it is used in many device applications such as solar cell, gas sensors, catalysts and electro-chromic devices (Mittiga *et al.*, 2006; Tanaka *et al.*, 2005).

CuO thin films can be prepared by numerous techniques such as activated reactive evaporation, thermal oxidation, vacuum evaporation, chemical vapor deposition, sol–gel process, electro-deposition and sputtering (Fernando, Wetthasinghe, 2000; Ray, 2001).

1.3. Doping of thin films

Doping is the addition of foreign atom into thin films. It could change or ameliorate the properties of thin films (Bugainovic *et al.*, 2009). The added element to the thin film is usually of small percentage, this is the cause that doping is considered as impurity.

From previous studies, different impurities, such as chromium (Cr), iron (Fe), silver (Ag), Sulfur (S), etc., were added to copper oxide thin films, which acquired new specifications or gained useful properties for different applications (Biccari, 2009).

In this study, Lithium (Li) was chosen to dope with CuO thin films because Li can enhance the filling of holes and improve the growth factor. In addition, it can reduce the band gap energy of CuO thin films, so increasing the ability of CuO thin films to absorb more solar light energy to be more useful in solar cell fabrication (Ray, 2001).

2. Materials and methods

2.1. CuO thin film preparation

Li-doped CuO thin films were prepared by sol gel deposition method. Spin coater (Mode: CY-SP4, voltage: 230 V and 60 Hz with vacuum pump), Magnetic stirrer (MS-H280-Pro LED-Digital Hotplate Stirrer) and Horizontal tube furnace (Model: DT-1400T, 1300°C) were used.

Copper (II) chloride dehydrate was dissolved in methanol, then the solution was stirred for 3 hours at 65°C. Trimethylamine was added as stabilizer. The mixture was left at room temperature for one day. Lithium chloride monohydrate was the source of Lithium. It was dissolved in methanol, then dropped to the mixture in 3 ratios of 1%, 2% and 4%. Therefore, three coating solutions of different Li ratio were obtained.

The host glass substrates were well cleaned using methanol, acetone and ultrasonic cleaner. Then, they were properly dried.

The prepared coating solutions were dropped carefully on the glass substrates, then rotated at 3000 rpm for 40 s and finally dried in a furnace at 350°C for 10 min to remove any unwanted chemical residuals.

2.2. Ultrasonic equipment

The ultrasonic equipment used in this study consisted of the following:

- Oscilloscope (54615B – HP) – used to obtain the transit time (t) travelling through specimen.
- Flaw detector (USIP 20 – Krautkramer Branson) – used to display pulse echo.
- Vector Signal Analyzer (89441A – HP – used to display echo signal profile of the used transducers.
- Normal transducers:
  1) 1 MHz transducer (Karl Deutsch S12 HB 1) of diameter 12 mm;
  2) 2 MHz transducer (Karl Deutsch S12 HB 2) of diameter 12 mm.
- Shear transducer: 2 MHz transducer (Karl Deutsch, MB 2y) of diameter 12 mm.
- Step blocks (VI and VII) – used as reference blocks; they had known thickness and ultrasonic velocity. They were used in calibration for knowing thickness accuracy.
- Water gel – used as coupling material.

2.3. Transducer modification

Normally, thin films have so small scale (from few nanometers (nm) to few micros (μm)). Therefore, amelioration of ultrasonic transducer had been done to focus ultrasonic waves, decreasing beam scattering and overcome the dead zone of the transducer. All these last purposes were done by using wedges.

A conical wedge was put in front of the transducer to make the transducer's front like the tip of a pen. Detection by focusing the ultrasonic waves in point

is more precise technique to pick up echoes from every point displacement over the specimen under test (Fig. 1).

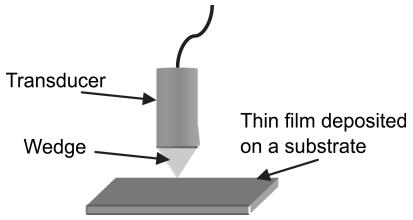

Fig. 1. Sketch of ultrasonic measurement using wedge.

The wedges were fabricated from glass, which was easy to handle and shaped. Glass wedges were as glass substrate, to fulfill impedance matching. The designed wedges took the form of a cone. The base of the wedges' cone had the same diameter (12 mm) as the transducers used in the study, but the tip (head) of the wedges had 2 mm diameter (Fig. 2). The base and the tip of the fabricated wedges were circular.

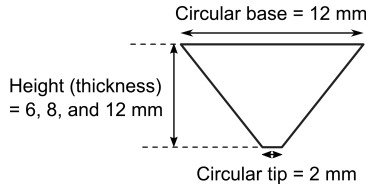

Wedges notation	Thickness [mm]
W_1	6
W_2	8
W_3	12

Fig. 2. Wedge shape and dimensions.

In previous study (Al-Shomar *et al.*, 2017), a delay line was developed, that had the same shape of the specimen under test, to overcome the dead zone of the transducer. In the present study, wedges were developed to act as delay line and as collimator of ultrasonic waves (Fig. 3).

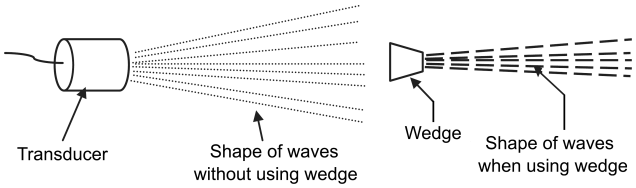

Fig. 3. Principle of wedge.

2.4. Optical equipment

The optical measurements were carried out by means of spectrophotometer apparatus (UV-3101PC – Serial No. A13 -29030002 – Shimadzu). These measurements undergo the band gap energy (E_g) determination (Oluyama *et al.*, 2014).

3. Results and discussion

3.1. Ultrasonic mode operation

Pulse echo technique was preferred to be used rather than other methods such as transmission method. In pulse echo technique one transducer can be used. This transducer has dual function, it transmits and receives pulse echo, thus providing easy way of test and reducing errors of measurements (ASTM E114-15, 2015).

3.2. Ultrasonic coupling

Any little bit air between the transducer and the specimen under test may cause ultrasonic waves dissipation. To eliminate air between the transducer and the specimen under test, coupling material (e.g. oil, water gel) must be present between them (Prokop *et al.*, 2003).

Coupling material acts as conductive medium that performs a close bond between the transducer and the specimen under test. Therefore, the type of coupling material must be chosen properly to enable such work.

There are some conditions to choose the coupling material:

1) It must not be absorbed by the specimen under test.
2) It must not change the chemical properties of the specimen under test.
3) It must not change the physical characterization of the specimen under test.
4) It must not harm the transducer or the specimen under test (i.e. it must not cause surface scratching, corrosion, etc.).
5) It must be as a lubricant for easy movement of the transducer on the specimen.
6) It must be of very few drops for preventing scattering of ultrasonic waves.
7) It must be of suitable material to allow high waves transmission through specimen.
8) It must be of low cost because it is consumed quickly.

It was found that water gel is the most suitable coupling material that fulfills all last cited conditions. In this study, water gel was put between the transducer front and the wedge base; also it was put between the wedge tip and the thin film specimen surface. Very few drops of water gel were used, just to prevent air but not affecting waves' transmission or measurements.

3.3. Ultrasonic transducers selection and calibration

From previous study, the suitable ultrasonic transducers to investigate oxide semiconductor thin films are ranged from 0.5 to 2 MHz (Al-Shomar *et al.*, 2017).

Table 1. Nominal and operating transducers frequencies.

Transducer type	Nominal frequency f [MHz]	Operating frequency f_o [MHz]	Deviation percentage
Normal (Karl Deutsch, S12 HB 1)	1	1.10	10%
Normal (Karl Deutsch, S12 HB 2)	2	2.30	15%
Shear (Karl Deutsch, MB2y)	2	2.44	22%

In this study, normal transducers of 1 and 2 MHz were used; in addition shear transducer of 2 MHz was used.

The used normal and shear transducers were calibrated according to DIN EN 10308 (Deutsch Norm, 2002). Table 1 shows the nominal and the operating transducers frequencies. Noting that the nominal frequency (f) is the frequency written on the transducer's piece, while the operating frequency (f_o) is the frequency measured after calibration.

The accuracy of transducers calibration measurements was about 0.04%.

Table 1 shows the deviation percentage between the nominal frequencies of the used transducers and their operating frequencies. The deviation percentage was taken into consideration when doing measurements and calculations.

3.4. Wedges effects on transducers performance

3.4.1. Transducer Near Field (NF)

The transducer near field is one of the important factors that can reflect the amelioration of the used transducers after using wedges. If the NF becomes smaller, the transducer's sensitivity becomes higher.

Near field, *NF* is given by the following formula (Al-Shomar *et al.*, 2017):

$$NF = (D_{\text{eff}})^2 \cdot \frac{f_o}{4C}, \tag{7}$$

where D_{eff} is the transducer's effective diameter, f_o is the operating frequency of the used transducer and C is the ultrasonic velocity in the prepared CuO thin films.

For undoped CuO thin films, the measured longitudinal velocity (C_L) was 4920 m/s, while the measured shear velocity (C_s) was 2260 m/s.

The near field, *NF* for the used transducers was shown in Table 2.

The transducers' diameter was reduced to be as the wedge tip diameter (2 mm) because the echoes were generated from this new diameter and entering the tested thin films. Therefore, the used transducers – with wedges – had new near fields. From Table 2, it was deduced that the wedge caused the reduction in the near field (dead zone) of the used transducers by about 97%. Thus, the used transducers – with wedges – became more suitable to study thin films: the dead zone (blind area) was reduced, the transducers became high sensitive and they had more suitable band to pick echoes easily.

Table 2. Near Field (*NF*) for the used transducers.

Transducer type	Near Field *NF* [mm]	
	Without wedge	With wedge
Normal (Karl Deutsch, S12 HB 1)	8.049	0.224
Normal (Karl Deutsch, S12 HB 2)	16.829	0.467
Shear (Karl Deutsch, MB2y)	38.867	1.080

3.4.2. Beam diameter (BD)

Beam diameter (*BD*) must be calculated to know the effect of wedge on beam collimation and scattering.

Beam diameter (*BD*) can be calculated as follow (Al-Shomar *et al.*, 2017):

$$BD\,(-6\text{ dB}) = 1.2\frac{FC_{\text{thin film}}}{f_o}D_{\text{eff}} = 0.2568 D_{\text{eff}} SF, \tag{8}$$

where BD – beam diameter, F – focal length, D_{eff} – effective transducer's diameter, fo – operating frequency, SF – normalized focal length ($= F/NF$), and $C_{\text{thin film}}$ – thin film velocity (longitudinal or shear).

By definition, the focal length of a transducer is the distance from the face of the transducer to the point in the sound field where the signal with the maximum amplitude is located (Birks *et al.*, 1991). Without using wedges, the focal length F is approximately equivalent to the transducers near field length that was calculated without wedges. While, when using wedges, the focal length F is approximately equivalent to the near field that was calculated with wedges.

Table 3 shows the reduction of the beam diameter while using wedges. Small beam diameter increases the transducer's sensitivity to detect flaws (Barakat, Afifi, 2011). Therefore, it can be said that the used

Table 3. Beam diameter (BD) for the used transducers.

Transducer type	Beam diameter BD [mm]	
	Without wedge	With wedge
Normal (Karl Deutsch, S12 HB 1)	3.0600	0.511
Normal (Karl Deutsch, S12 HB 2)	3.1990	0.533
Shear (Karl Deutsch, MB2y)	3.0599	0.510

transducers were ameliorated by wedges and their sensitivity was increased.

3.4.3. Beam directivity (D)

Beam directivity can reflect good information for the effect of wedge on transducers.

The divergence angle θ (½ the beam spread angle) represents a measure from the center of the acoustic axis to the point where the sound pressure decreased by one half (−3 dB) to the side of the acoustic axis in the far field (IEEE, 1997). The divergence angle θ was from echo signal profile of the used transducers using Vector Signal Analyzer (89441A, HP).

For a transducer of a conical beam, the directivity D can be calculated as follow (IEEE, 1997):

$$D = \frac{2}{1 - \cos\frac{\theta}{2}}. \tag{9}$$

Three models of wedges were fabricated (W_1, W_2, and W_3); they had the same base as the transducers' front diameter (12 mm), also they had same tip (2 mm) but they differed in height (= thickness) (6, 8 and 12 mm). From Table 4, it can be noticed that, when using wedges the directivity was improved and wedge of biggest height (W_3 = 12 mm) had directivity ranging from 1.06 to 1.17. This means that the higher wedge produced a uniform response for directivity. The results agreed with that given by Rus *et al.* (2004).

Table 4. Beam directivity, D.

Transducer type	Beam directivity, D			
	Without wedge	With wedge		
		W_1	W_2	W_3
Normal (Karl Deutsch, S12 HB 1)	1.35	1.23	1.22	1.17
Normal (Karl Deutsch, S12 HB 2)	1.01	1.11	1.09	1.07
Shear (Karl Deutsch, MB2y)	1.55	1.08	1.07	1.06

3.4.4. Reflection (R_1) and transmission (T_1) of transducers' waves

When a wedge was inserted between the transducer and the test specimen (CuO thin films), the ultrasonic waves were transmitted and reflected through the three media: transducer, wedge and test specimen.

The intensity transmission and intensity reflection coefficient, T_1 and R_1 respectively are given in Eqs. (10) and (11) (Rose, Meyer, 1974).

$$T_1 = \frac{4}{2 + \left(\frac{Z_3}{Z_1} + \frac{Z_1}{Z_3}\right)\cos^2 k_2 d + a^*}, \tag{10}$$

$$R_1 = 1 - T_1, \tag{11}$$

where

$$a^* = \left(\frac{Z_3^2}{Z_1 Z_3} + \frac{Z_1 Z_3}{Z_2}\right)\sin^2 k_2 d$$

and Z_1, Z_2, Z_3 are the characteristic acoustic impedances of the three media respectively, k_2 is the wave number in the wedge and d is the wedge's thickness (= height).

The influence of different wedges' thicknesses is tabulated in Table 5. Wedges' thicknesses affected the transmission and reflection of ultrasonic waves. T_1 was decreased as wedge's thickness increased, while R_1 did the opposite. The ultrasonic waves' path was smaller in 6 mm wedge thickness so the waves' transmission was high. While, the ultrasonic waves' path was higher in 8 and 12 mm wedge thicknesses, the waves' transmission was lower.

Table 5. Intensity transmission T_1 and intensity reflection R_1 coefficients variation with different wedge's thickness.

Wedge's thickness d [mm]	T_1 [%]	R_1 [%]
6	18.935	81.064
8	15.942	84.058
12	12.112	87.890

3.5. Ultrasonic velocity measurements for CuO doped thin films

The ultrasonic velocities (longitudinal (C_L) and shear (C_s)) were measured according to formula (1). The estimated accuracy percent of measuring ultrasonic velocities was 0.05%.

The measured ultrasonic longitudinal and shear velocities were increased as the percentage of Li increased in the doped CuO thin films (Fig. 4). More Li percentage caused more CuO gap filling. Therefore, there was a decrement in the time of beam travelling across the films molecules, thus the ultrasonic velocities increased. 4% Li-CuO thin films was the most films that had highest ultrasonic velocities.

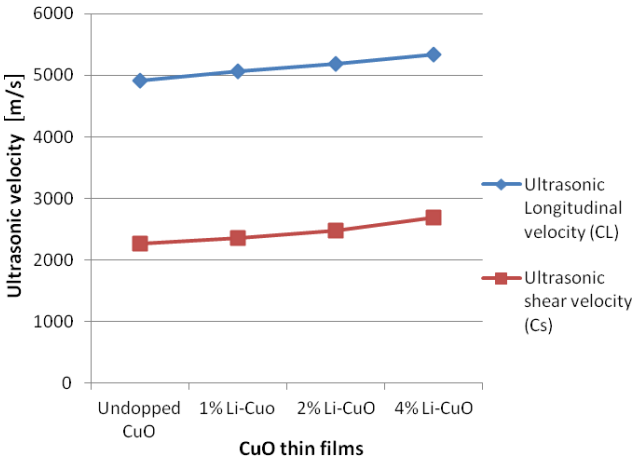

Fig. 4. Ultrasonic velocities measurement for different CuO thin films with different Li concentration.

3.6. Thin films thickness measurements using ultrasonic

Using pulse echo technique, the thickness d of the prepared thin films can be obtained following formula (1) (Fig. 5).

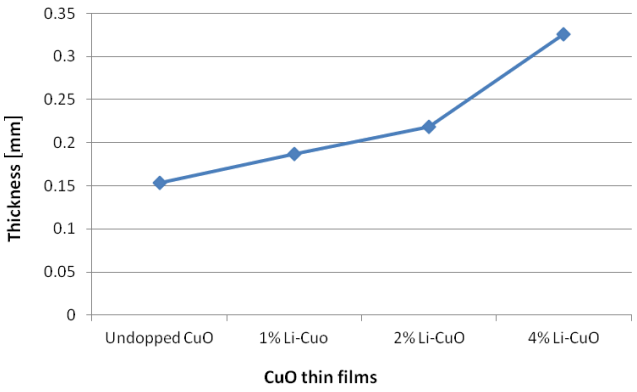

Fig. 5. Thin films thickness measurement for different CuO thin films with different Li concentration.

The thickness measurements were carried out several times for each prepared specimen and then the average value was taken. The deviation of measurements was about ±0.008 mm.

Figure 5 shows that the thicknesses of the doped specimens was increased as the Lithium (Li) percentage was increased. This may be due to the increment of CuO grain size because Li enhanced the grain growth of CuO thin films (Al-Shomar *et al.*, 2017). 4% Li-CuO thin films was the most films that had highest thicknesses.

3.7. Density (ρ) measurement

The density ρ of the prepared specimens was measured by the difference in weights that were measured in air and in water (Fig. 6).

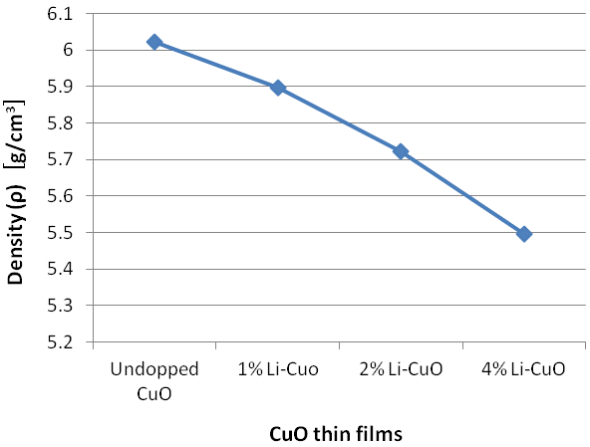

Fig. 6. Density ρ measurement for different CuO thin films with different Li concentration.

The density ρ measurements were carried out several times for each prepared specimen and then the average value was taken. The deviation of measurements was about ±0.001 g/cm^3.

Figure 6 shows slight decrement of the density ρ with respect to the increment in Li content. This may referred to CuO thin films undergo volume increment as the Li percentage increased, due to increment in growth rate. Knowing that the density ρ is inversely proportional to the volume from the reputable formula: ρ = mass/volume.

3.8. Elastic moduli measurements using ultrasonic

The elastic moduli (longitudinal L, shear G, bulk K, and Young's E) describe the elastic properties of a given material. The elastic properties can give information about material's rigidity. Rigid objects such as an iron nail have strong interatomic forces and rigid lattice, thus they have considerably low elastic moduli. Not rigid objects such as rubber gloves have less rigid lattice, their atoms are aligned in long flexible molecular chains, each chain being only loosely bound to its neighbors, so they have considerably high elastic moduli (Halliday *et al.*, 2008).

Using formulas (1)–(4) and (6) the longitudinal velocity C_L, shear velocity C_S and elastic moduli (longitudinal L, shear G, bulk K, and Young's E) variation with respect to Lithium (Li) concentration were calculated, Fig. 7. The elastic moduli measurements were carried out several times for each prepared specimen and then the average value was taken. The deviation of measurements was about ±0.04 GPa.

Figure 7 shows the increments of the elastic moduli (longitudinal L, shear G, bulk K, and Young's E) with the increment of Li content in the CuO thin films. Thus, it can be said that the doped CuO thin films gained flexibility when doping with Li and this flexi-

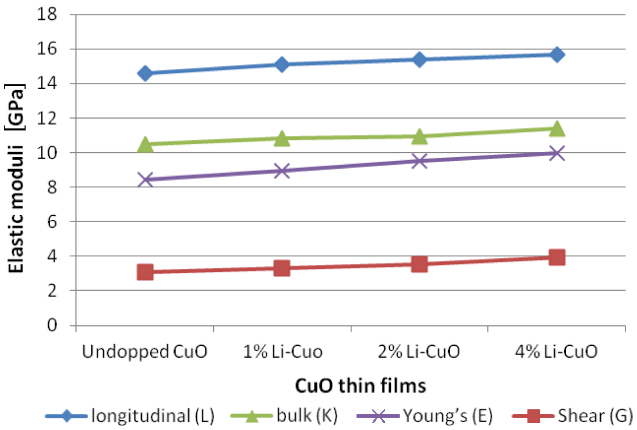

Fig. 7. Elastic moduli (longitudinal L, shear G, bulk K, and Young's E) variation with respect to Lithium (Li) concentration.

bility increased as the Li content increased. 4% Li-CuO thin films was the most films that had highest elastic moduli.

3.9. Poisson's ratio v measurement using ultrasonic

Using formula (4), Poisson's ratio v was calculated. Figure 8 shows the variation of Poisson's ratio v with respect to Li concentration in the prepared CuO thin films.

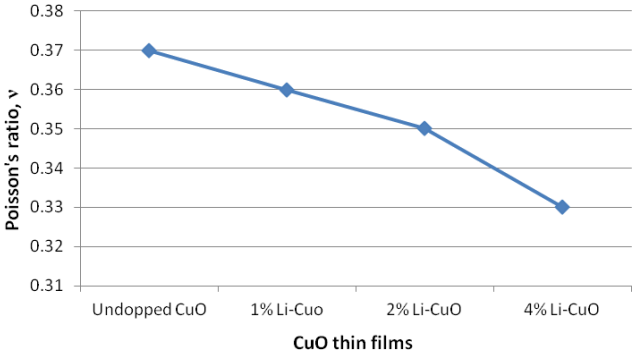

Fig. 8. Variation of Poisson's ratio v with respect to Li concentration in CuO thin films.

Poisson's ratio v measurements were carried out several times for each prepared specimen and then the average value was taken. The deviation of measurements was about ± 0.009.

Poisson's ratio v is affected by the changes in the cross-link density of the molecular network. The undoped CuO thin films had Poisson's ratio $v = 0.37$, so they were considered to have low cross-link density, because their Poisson's ratio (v) was between 0.3 and 0.4. Li-CuO thin films had Poisson's ratio v ranged from 0.33 to 0.36. Li caused a considerable increment in the cross-link density of CuO thin films. But Li content may be not sufficient to greatly increase the cross-link density of the prepared CuO thin films. 4% Li-CuO thin films was the most films that had the lowest Poisson's ratio v value.

3.10. Band gap energy E_g measurements

Band gap energy E_g was determined by optical method, different specimens of undoped and Li-doped CuO thin films were measured in the wavelength range of 400 to 1100 nm. E_g can be calculated using the following formula (Halliday *et al.*, 2008):

$$E_g = hf, \tag{12}$$

where f is the frequency and h is the Planck's constant ($\approx 6.626 \cdot 10^{-34}$ J $\cdot$ s $\approx 4.1357 \cdot 10^{-15}$ eV $\cdot$ s).

Table 6. E_g measurements from ultrasonic and from optical methods.

Specimen	E_g [eV] (± 0.02 eV)
Undopped CuO	1.30
1% Li-CuO	1.21
2% Li-CuO	1.14
4% Li-CuO	1.06

The knowledge of the band gap energy E_g is very useful to have information about the specimen's microstructure (Rajendran *et al.*, 2003). In previous study (El-Mallawany, 1998), band gap energy E_g calculated for thin films can give information about their improvement, i.e. decrement in E_g reflects increment in the thin films' improvement. Table 6 shows the decrement of the band gap energy E_g with the increment of Lithium (Li) concentration in the prepared CuO thin films. E_g was decreased from 1.3 eV to 1.06 eV. Li filled the molecular network of the prepared CuO thin films and by increasing its concentration the intermolecular gap decreased, causing the decrement in the band gap energy. Therefore, it can be said that Li upgraded the prepared CuO thin films to be more applicable in solar cells fabrication. Li doped CuO thin films could be considered as good absorber layer in hetero-junction solar cell (Dahrul *et al.*, 2018). 4% Li-CuO was the most suitable films that had the lowest band gap energy E_g.

4. Conclusion

By employing the ameliorated transducers using the fabricated wedge, the measurements became more accurate and easier. The wedge acted both as delay line to overcome the transducer's blind area and as collimator to collect ultrasonic waves in point. The main advantages of these wedges were:

1) overcoming the blind area of the transducer (i.e. the transducer near field (NF) decreased when using wedges),

2) decreasing the beam diameter to increase transducer's sensitivity,
3) enhancing beam directivity and beam transmission through thin films specimens,
4) making the transducer more useful in measuring thin specimens. Therefore, it can be said that ultrasonic method is an easy, safe and fast method to study thin films.

The band gap energy E_g – measured by optical method – was decreased as Li content increment in CuO thin films.

In addition, using ultrasonic, thin films' properties can be easily determined: like thickness, elastic moduli and Poisson's ratio that reflected good idea about films' variation with Li percentage.

Finally, the study deduced that Li doping caused the improvement of CuO thin films to be used as absorber layer in hetero-junction solar cell. Li-doped CuO thin films could have more efficiency to absorb solar light. Results concluded that 4% Li-CuO thin films was the most suitable films that had good properties to be used in solar cell fabrication.

References

1. Al-Shomar S.M., Barakat M.A.Y., Mahmoud S.A. (2017), *Modified ultrasonic technique to study Gd-doped ZnO films*, MAPAN-Journal of Metrology Society of India, **32**, 2, 121–126, doi: 10.1007/s12647-016-0199-8.
2. ASTM E114-15 (2015), *Standard practice for ultrasonic pulse-echo straight-beam contact testing*, ASTM International, West Conshohocken, PA.
3. Barakat M.A., Afifi H.A.A. (2011), *The use of ultrasound to detect subsurface defects in aluminum pieces*, Journal of Physical Science and Application, **1**, 1, 29–36.
4. Biccari F. (2009), *Defects and doping in Cu_2O*, Ph.D. Thesis, Sapienza – University of Rome.
5. Birks A.S., Green R.E., McIntire P. (1991), *Nondestructive testing handbook. Vol. 7, Ultrasonic testing*, American Society of Nondestructive Testing, Columbus, OH.
6. Bugainovic S.J., Grekulovic V.J., Rajcic-Vujasinovi M.M., Stevic Z.M., Stankovic Z.D. (2009), *Electrochemical synthesis and characterization of copper (I) oxide* [in Serbian], Hemijska Industrija, **63**, 3, 201–2017, ISSN 0367-598X.
7. Chopra K.L., Paulson P.D., Dutta V. (2004), *Thin-film solar cells: an overview*, Progress in Photovoltaics: Research and Applications, **12**, 69–92.
8. Dahrul M., Alatas H., Irzaman (2016), *Preparation and optical properties study of CuO thin film as Applied solar cell on LAPAN-IPB satellite*, Procedia Environmental Sciences, **33**, 661–667.
9. Deutsch Norm (2002), *Nondestructive testing. Ultrasonic testing of steel bars*, DIN EN 10308.
10. El-Mallawany R. (1998), *Tellurite glasses part 1. Elastic properties*, Materials Chemistry and Physics, **53**, 93–120.
11. Fernando C.A.N., Wetthasinghe S.K. (2000), *Investigation of photoelectrochemical characteristics of n-type Cu_2O films*, Solar Energy Materials and Solar Cells, **63**, 3, 299–308.
12. Forsyth J.B., Hull S. (1991), *The effect of hydrostatic pressure on the ambient temperature structure of CuO*, Journal of Physics: Condensed Matter, **3**, 28, 5257–5261.
13. Gaafar M.S., El-Wakil A.A., Barakat M.A. (2013), *Study of the effect of radiation and frequency on the electrical properties and ultrasonic properties of polyethylene*, Archives of Applied Science Research, **5**, 2, 158–166.
14. Halliday D., Resnick R., Walker J. (2008), *Fundamentals of physics. Extended*, 8th Ed., John Wiley & Sons, Inc., ISBN 978-0-471-75801-3.
15. IEEE (1997), The IEEE standards dictionary of electrical and electronics terms, 6th Ed., New York, ISBN 1-55937-833-6.
16. Katz E.A., Faiman D., Lyubin V. (2002), *Persistent internal photopolarization in C60 thin-films: proposal for a novel fullerene – based solar cells*, Conference Digest of the 29th IEEE Photovoltaic Specialist Conference, New Orleans, May 19–24, pp. 1298–1301.
17. Matori K.A., Zaid M.H.M., Sidek H.A.A., Halimah M.K., Wahab Z.A., Sabri M.G.M. (2010), *Influence of ZnO on the ultrasonic velocity and elastic moduli of soda lime silicate glasses*, International Journal of the Physical Sciences, **5**, 14, 2212–2216.
18. Mittiga A., Salza E., Sarto F., Tucci M., Vasanthi R. (2006),*Heterojunction solar cell with 2% efficiency based on a Cu_2O substrate*, Applied Physics Letters, **88**, 16, 163502.
19. Oluyama S.S., Nyagba M.S., Ojo A.S. (2014), *Optical properties of copper (I) oxide thin films synthesized by SILAR technique*, IOSR Journal of Applied Physics, **6**, 3, 102–105.
20. Prokop A.F., Vaezy S., Noble M.L., Kaczkowski P.J., Martin R.W., Crum L.A. (2003), *Polyacrylamide gel as an acoustic coupling medium for focused ultrasound therapy*, Ultrasound in Medicine and Biology, **29**, 9, 1351–1358.
21. Rajendran V., Palanivelu N., Chaudhuri B.K., Goswami K. (2003), *Characterisation of semiconducting V_2O_5-Bi_2O_3-TeO_2 glasses through ultrasonic measurements*, Journal of Non-Crystalline Solids, **320**, 1–3, 195–209.
22. Ray S.C. (2001), *Preparation of copper oxide thin film by the sol-gel-like dip technique and study of their structural and optical properties*, Solar Energy Materials and Solar Cells, **68**, 3–4, 307–312.

23. Richardson T.J., Slack J.L., Rubin M.D. (2001), *Electrochromism in copper oxide thin films*, Electrochimica Acta, **46**, 13–14, 2281–2284.

24. Rose J.L., Meyer P.A. (1974), *Ultrasonic signal-processing concepts for measuring the thickness of thin layer*, Materials Evaluation, **32**, 2, 249–225.

25. Rus G., Wooh S.-C., Gallego R. (2004), *Analysis and design of wedge transducers using the boundary element method*, Journal of the Acoustical Society of America, **115**, 6, 2919–2927.

26. Saravanakannan V., Radhakrishnan T. (2014), *Structural, electrical and optical characterization of CuO thin films prepared by spray pyrolysis technique*, International Journal of ChemTech Research, **6**, 1, 306–310.

27. Tanaka H., Shimakawa T., Miyata T., Sato H., Minamia T. (2005), *Effect of AZO film deposition conditions on the photovoltaic properties of AZO-Cu_2O heterojunctions*, Applied Surface Science, **244**, 1–4, 568–572.